ScienceDirect

IFAC PapersOnLine CONFERENCE PAPER ARCHIVE

IFAC PapersOnLine 51-26 (2018) 155–160

A TP-LPV-LMI based control for Tumor Growth Inhibition ⋆

Levente Kovács *, **György Eigner** *

* *Physiological Controls Research Center and Research, Innovation, and Service Center, Óbuda University, Budapest, Hungary (e-mail:{kovacs.levente, eigner.gyorgy}@nik.uni-obuda.hu).*

Abstract: The paper investigates the applicability of an advanced modern control method related to control of tumor growth under angiogenic inhibition. In order to describe the physiological process, a simple mathematical model was applied consisting of two states, the volume of the tumor and the inhibitor value. Extended Kalman Filter (EKF) was applied to estimate the unmeasurable state (inhibitor level). Linear Parameter Varying (LPV) models are used both at controller design (difference based control oriented LPV model) and EKF development (LPV model) level as well. We have used the Tensor Product (TP) model transformation accompanied by Linear Matrix Inequality (LMI) based optimization method in order to design a Parallel Distributed Compensator (PDC) kind TP-LPV-LMI controller considering additive disturbances (on both states) and sensor noise as well. Despite the assumed unfavorable effects the TP-LPV-LMI controller performed well achieving low final tumor volume and less totally injected inhibitor level.

Keywords: Extended Kalman Filter, Linear Parameter Varying Control, Linear Matrix Inequality, Tensor Product, Tumor Growth Control

1. INTRODUCTION

Targeted Molecular Therapies (TMTs) are recently developed innovative cancer treatment opportunities and can be applied for more personalized therapy regarding cancer provision. The aim of TMTs is to inhibit a given biological mechanisms of the cancer, Charlton and Spicer (2016). Compared to the classical treatments – e.g. chemotherapy, radiotherapy, surgical intervention – the TMTs are less harmful; moreover, their specificities allow targeting directly important mechanisms of the tumor, Xing and Lisong (2017).

The current study focuses on a specific TMT, the control of tumor growth by angiogenic inhibition, i.e. blocking blood vessel formation in the tumor. The phenomena is connected to a well-known property of tumors: beyond a certain level due to the lack of nutrients tumors can grow only by creating own blood vessels. The dominant way to form own vessels is the production of angiogenic factors (signal transducers) – the so-called vascular endothelial growth factor (VEGF) – by which they can catalyze the formation of new blood vessels, Vasudev and Reynolds (2014). In order to "tame" the given tumor it is possible to inhibit this phenomena causing the "starvation" of the tumor and inhibiting its growing. One of the mostly used angiogen inhibitor is the bevacizumab (avastin) Abdalla et al. (2018), considered for this study as well.

The physiological process of angiogenesis can be modeled and controlled by control engineering methods. The main goal of the therapy is to reach the smallest tumor volume by using as small amount of drug as possible. Many investigations have been done in the last decade to analyze the problem and provide some solution: Sápi (2015); Lobato et al. (2016); Drexler et al. (2017b); Klamka et al. (2017); Drexler et al. (2017c,d). However, there are still open questions to be answered like handling the nonlinearities or parameter uncertainties.

One possible solution is the application of LPV framework, since it allows the use of linear control techniques by effective handling of nonlinearities; moreover, the parameter uncertainties can be handled as well (White et al. (2013); Kovács (2017)). In addition, a useful technique is the TP model transformation, which is able to represent the LPV functions (and systems) as TP models optimizing the LPV vertex. During the transformation, the goals of the control can be formulated via LMIs and the processes can be executed together leading to a TP-LPV-LMI controller (Boyd et al. (1994); Kuti et al. (2017b); Baranyi et al. (2013)).

The current study points out an LPV-based solution for a novel model (Drexler et al. (2017a,c,d)) in control oriented form. The framework effectively handles the nonlinearity and parameter uncertainty being comparable with the classical robust control solutions (Sápi (2015)).

The paper is structured as follows: first, the applied mathematical model and the developed LPV models are introduced. This is followed by the controller design steps including the TP model transformation, LMI formulations

⋆ Gy. Eigner was supported by the ÚNKP-17-4/I. New National Excellence Program of the Ministry of Human Capacities. This project has received funding from the European Research Council (ERC) under the European Union's Horizon 2020 research and innovation programme (grant agreement No 679681).

10.1016/j.ifacol.2018.11.146

and EKF design. The third part presents our findings discussing the research results. Finally, we conclude our work and formulate further research direction possibilities.

2. MATHEMATICAL MODELS

2.1 Tumor Growth Model

In this study we have investigated the tumor growth model proposed by Drexler et al. (2017a,c,d). The model consists of two state variables: the $x_1(t)$ [mm^3] tumor volume and the $x_2(t)$ [mg/kg] angiogen inhibitor level in the blood. The mathematical formulation is described by:

$$\begin{aligned} \dot{x_1}(t) &= ax_1(t) - bx_1(t)x_2(t) \\ \dot{x_2}(t) &= -cx_2(t) + u(t) \end{aligned} . \tag{1}$$

The measurable output of the model is $x_1(t)$, while the input of the model is the $u(t)$ [mg/kg]/day] inhibitor. The considered parameters of the model are the $a = 0.27$ [1/day] growing rate, the $b = 0.0074$ [kg/mg/day] inhibitor rate and $c = \ln(2)/3.9$ [1/day] as the inhibitor clearance rate determined by parametric identification based on mice experiments regarding to C38 colon adenocarcinoma (Drexler et al. (2017a)). One can observe that $x_1(t)$ is limitlessly growing by the a scaling factor without inhibition. The steady-state of the model is:

$$\begin{aligned} 0 &= ax_{1,\infty} - bx_{1,\infty}x_{2,\infty} \\ 0 &= -cx_{2,\infty} + u_\infty \end{aligned} . \tag{2}$$

It can be seen from (2) that $x_{2,\infty} = a/b$ and $u_\infty = c \cdot a/b$ are not dependent from $x_{1,\infty}$. Hence, $x_{2,\infty} = a/b$ is needed in order to keep permanent tumor volume which requires $u_\infty = c \cdot a/b$ from the input side. In order to decrease the tumor volume, $u_\infty > c \cdot a/b$ is needed leading to $x_{2,\infty} > a/b$.

2.2 LPV Model Development

A general LPV model can be described in state-space form as follows (Sename et al. (2013); White et al. (2013)):

$$\begin{aligned} \dot{\mathbf{x}}(t) &= \mathbf{A}(\mathbf{p}(t))\mathbf{x}(t) + \mathbf{B}(\mathbf{p}(t))\mathbf{u}(t) \\ \mathbf{y}(t) &= \mathbf{C}(\mathbf{p}(t))\mathbf{x}(t) + \mathbf{D}(\mathbf{p}(t))\mathbf{u}(t) \\ \begin{pmatrix}\dot{\mathbf{x}}(t)\\ \mathbf{y}(t)\end{pmatrix} &= \mathbf{S}(\mathbf{p}(t)) \begin{pmatrix}\mathbf{x}(t)\\ \mathbf{u}(t)\end{pmatrix} \\ \mathbf{S}(\mathbf{p}(t)) &= \begin{bmatrix}\mathbf{A}(\mathbf{p}(t)) & \mathbf{B}(\mathbf{p}(t))\\ \mathbf{C}(\mathbf{p}(t)) & \mathbf{D}(\mathbf{p}(t))\end{bmatrix} \end{aligned} . \tag{3}$$

In this structure, $\mathbf{A}(t) \in \mathbb{R}^{n\times n}$, $\mathbf{B}(t) \in \mathbb{R}^{n\times m}$, $\mathbf{C}(t) \in \mathbb{R}^{k\times n}$ and $\mathbf{D}(t) \in \mathbb{R}^{k\times m}$ are the state, input, output and feed-forward matrices, while $\mathbf{x}(t) \in \mathbb{R}^n$, $\mathbf{y}(t) \in \mathbb{R}^k$ and $\mathbf{u}(t) \in \mathbb{R}^m$ are the state, output and input vectors, respectively. The $\mathbf{S}(\mathbf{p}(t)) \in \mathbb{R}^{(n+k)\times(n+m)}$ represents the system matrix – which is the LPV function at the same time. The matrices are $\mathbf{p}(t)$ dependent, where $\mathbf{p}(t)$ is the parameter vector of the scheduling variables $p_i(t)$, namely, $\mathbf{p}(t) = [p_1(t) \dots p_R(t)]$. The $\mathbf{p}(t) \in \mathbf{\Omega}^R \in \mathbb{R}^R$, where $\mathbf{\Omega} = [p_{1,min}, p_{1,max}] \times [p_{2,min}, p_{2,max}] \times \dots \times [p_{R,min}, p_{R,max}] \in \mathbb{R}^R$.

We have used the (3) representation during the LPV model development. Two LPV models have been developed: one for control design purposes and the other one for the EKF design. Hence, we denoted their parameter vectors as $\mathbf{p}(t) \in \mathbb{R}^2$ and $q(t) \in \mathbb{R}^1$, respectively.

Model-A In case of the first LPV model, we have selected $q(t) = x_1(t)$ as scheduling variable from (1) through which the following LPV model can be obtained:

$$\begin{aligned} \dot{\mathbf{x}}(t) &= \mathbf{A}_A(q(t))\mathbf{x}(t) + \mathbf{B}_A\mathbf{u}(t) \\ \mathbf{y}(t) &= \mathbf{C}_A\mathbf{x}(t) \\ \mathbf{S}_A(q(t)) &= \begin{bmatrix}\mathbf{A}_A(q(t)) & \mathbf{B}_A\\ \mathbf{C}_A & 0\end{bmatrix} = \begin{bmatrix}a & -bq(t) & 0\\ 0 & -c & 1\\ 1 & 0 & 0\end{bmatrix} \end{aligned} , \tag{4}$$

where $\mathbf{B}_A = \mathbf{B} = [0\ 1]^\top$ and $\mathbf{C}_A = \mathbf{C} = [1\ 0]$. The $q(t) \in \{q_{min}, \dots, q_{max}\} \equiv \{10^{-3}, \dots, 5 \times 10^5\}$. The q_{min} is the approximation of the zero tumor volume. This is physiologically meaningful as to the target of TMTs is not to eliminate the tumor itself, but to "tame" it. The q_{max} is in accordance with our previous investigations (Sápi (2015)). Model-A has been used for the EKF design.

Model-B We have developed a difference based control oriented LPV model for controller design purposes. We aimed to apply PDC kind state-feedback control as it directly models the error to be eliminated and it is not necessary to apply reference compensation beside. In this case a simple state transformation have been applied: $\Delta x_1(t) = x_1(t) - x_{1,ref}(t)$, $\Delta x_2(t) = x_2(t) - x_{2,ref}(t)$ and $\Delta u(t) = u(t) - u_{ref}(t)$. The new state variables model the error dynamics, namely, they describe the deviation of the original states from given reference states. In this way, the reference for the control will be $\Delta\mathbf{r} = \mathbf{0}^{2\times1}$, which is equivalent with the zero deviation of the state variables of the original model from the state variables of the reference system. Hence, the aim of the control becomes $\Delta\mathbf{x}(t) = [x_1(t), x_2(t)]^\top$, namely, $\Delta\mathbf{x}(t) \to \mathbf{0}$, while $t \to \infty$. The transformation of (1) and the new model is described by:

$$\begin{aligned} &\Delta\dot{x}_1(t) = \dot{x}_1(t) - \dot{x}_{1,ref}(t) = \\ &ax_1(t) - bx_1(t)x_2(t) \\ &-\big(ax_{1,ref}(t) - bx_{1,ref}(t)x_{2,ref}(t)\big) = \\ &a\Delta x_1(t) - bx_1(t)x_2(t) + bx_{1,ref}(t)x_{2,ref}(t) + 0 = \\ &a\Delta x_1(t) - bx_1(t)x_2(t) + bx_{1,ref}(t)x_{2,ref}(t) \\ &+bx_1(t)x_{2,ref}(t) - bx_1(t)x_{2,ref}(t) = \\ &(a - bx_{2,ref}(t))\Delta x_1(t) - bx_1(t)\Delta x_2(t) \end{aligned} . \tag{5}$$

$$\begin{aligned} &\Delta\dot{x}_2(t) = \dot{x}_2(t) - \dot{x}_{2,ref}(t) = \\ &-cx_2(t) + u(t) - \big(-cx_{2,ref}(t) + u_{ref}(t)\big) = \\ &-c\Delta x_2(t) + \Delta u(t) \end{aligned}$$

The state-space description of (5) becomes as follows:

$$\begin{aligned} \Delta\dot{\mathbf{x}}(t) &= \mathbf{A}_B(\mathbf{p}(t))\Delta\mathbf{x}(t) + \mathbf{B}_B\Delta\mathbf{u}(t) \\ \Delta\mathbf{y}(t) &= \mathbf{C}_B\Delta\mathbf{x}(t) \\ \mathbf{S}_B(\mathbf{p}(t)) &= \begin{bmatrix}\mathbf{A}_B(\mathbf{p}(t)) & \mathbf{B}_B\\ \mathbf{C}_B & 0\end{bmatrix} = \\ &\begin{bmatrix}a - bp_1(t) & -bp_2(t) & 0\\ 0 & -c & 1\\ 1 & 0 & 0\end{bmatrix} \end{aligned} . \tag{6}$$

Here, $p_1(t) = x_{2,ref}(t) \in \{p_{1,min}, \dots, p_{1,max}\} \equiv \{a/b + 10^{-3}, \dots, 10^4\}$ and $p_2(t) = x_1(t) \in \{p_{2,min}, \dots, p_{2,max}\} \equiv \{10^{-3}, \dots, 5 \times 10^5\}$ – with $\mathbf{p}(t) = [p_1(t), p_2(t)]^\top$. $p_{1,min} = x_{2,ref,min} = a/b + 10^{-3}$ which is the approximation of a/b and needed to keep the controllability of the model. This is a consequence of (1), namely, the inhibitor level has to be higher than a/b in order to decrease the tumor volume. $p_{1,max}$ is selected based on previous investigations (Sápi (2015)), as the highest possible level of inhibitor. Since

$p_2(t)$ is basically the equivalent of $q(t)$, the $p_2(t) \equiv q(t) \in \{q_{min}, \dots, q_{max}\} \equiv \{10^{-3}, \dots, 5 \times 10^5\}$.

Remark 1. Model-A is used for EKF design while Model-B is applied for controller design. The starting model was the same on which simple algebraic transformation has been done regarding the control oriented LPV model. The separation of them from the global stability point of view did not cause instability issues.

3. CONTROLLER DESIGN

3.1 The TP Model Transformation

The TP model transformation allows to represent arbitrary LPV models by optimizing the polytopic space of the LPV model. The finite element convex polytopic TP model can be described as follows:

$$\begin{pmatrix}\dot{\mathbf{x}}(t)\\ \mathbf{y}(t)\end{pmatrix} = \mathbf{S}(\mathbf{p}(t)) \begin{pmatrix}\mathbf{x}(t)\\ \mathbf{u}(t)\end{pmatrix} \\ \mathbf{S}(\mathbf{p}(t)) = \mathcal{S} \overset{\mathrm{R}}{\underset{\mathrm{r=1}}{\boxtimes}} \mathbf{w}_r(p_r(t)) = \mathcal{S} \times_r \mathbf{w}(\mathbf{p}(t)) \quad . \tag{7}$$

The core tensor $\mathcal{S} \in \mathbb{R}^{I_1 \times I_2 \times \dots \times I_R \times (n+k) \times (n+m)}$ consists of $\mathbf{S}_{i_1,i_2,\dots,i_R}$ linear time invariant (LTI) systems – which are the vertices of the polytope. The $\mathbf{p}(t)$ dependent vector valued weighting function $\mathbf{w}_r(p_r(t))$ consists of $w_{r,i_r}(p_r(t))$ $(i_r = 1 \dots I_R)$ continuous convex weighting functions. The convexity criteria is satisfied, if $\forall r, i, p_r(t)$: $w_{r,i_r}(p_r(t)) \in [0,1]$ and $\forall r, p_r(t) : \sum_{i=1}^{I_r} w_{r,i_r}(p_r(t)) = 1$, which must be true during the application. We have used the Minimal Volume Simplex (MVS) convex hull representation (Kuti et al. (2017b)). By applying it, the TP model approximating the original model inside the Ω hypercube with given accuracy depends on the applied sampling resolution in Ω (Kuti et al. (2017a,b); Hedrea et al. (2017)). The necessary steps of the realization of the TP model transformation are available in Baranyi et al. (2013); Kuti et al. (2017a); Galambos and Baranyi (2015).

A state-feedback kind controller can be described as follows (White et al. (2013)):

$$\mathbf{u}(t) = -\mathbf{G}(\mathbf{p}(t))\mathbf{x}(t)\,. \tag{8}$$

The $\mathbf{G}(\mathbf{p}(t)) \in \mathbb{R}^{m \times n}$ is the parameter dependent controller gain. The TP-based state-feedback kind polytopic controller becomes:

$$\mathbf{G}(\mathbf{p}(t)) = \mathcal{G} \overset{\mathrm{R}}{\underset{\mathrm{r=1}}{\boxtimes}} \mathbf{w}_r(p_r(t)) = \mathcal{G} \times_r \mathbf{w}(\mathbf{p}(t))\,, \tag{9}$$

where $\mathcal{G}$ feedback tensor consists of $\mathbf{G}_{i_1,i_2,\dots,i_R}$ feedback gain matrices. Each $\mathbf{G}_i$ belongs to a given $\mathbf{S}_i$ vertex. The connection between them is characterized by the $\mathbf{w}_r(p_r(t))$, similar to (7). The resulting $\mathbf{G}(\mathbf{p}(t))$ controller is the convex combination of the gains $\mathbf{G}_i$ in the vertices.

3.2 Linear Matrix Inequality based Controller Design

A polytopic LPV system can be represented as $\dot{\mathbf{x}}(t) = \mathbf{A}(\mathbf{p}(t))\mathbf{x}(t) + \mathbf{B}(\mathbf{p}(t))\mathbf{u}(t)$, where the vertices of the polytope are $[\mathbf{A}(\mathbf{p}(t))\ \mathbf{B}(\mathbf{p}(t))] = \sum_{r=1}^{R} \mathbf{w}_r(\mathbf{p})[\mathbf{A}_r\ \mathbf{B}_r]$ and where $\mathbf{w}_r(\mathbf{p})$ is $\mathbf{p}$-dependent convex weighting function (Baranyi et al. (2013)). In accordance with Lyapunov's direct method, the Lyapunov function can be $V(\mathbf{x}(t)) = \mathbf{x}^\top \mathbf{P} \mathbf{x} = \mathbf{x}^\top \mathbf{X}^{-1} \mathbf{x}$, at which the a given controller candidate can be described as:

$$\mathbf{u}(t) = \mathbf{M}(\mathbf{p}(t))\mathbf{X}^{-1}\mathbf{x}(t) = \sum_{j=1}^{J} \mathbf{w}_j(\mathbf{p})\mathbf{M}_j\mathbf{X}^{-1}\mathbf{x}(t) \tag{10}$$

The derivative of the Lyapunov function becomes as follows:

$$\dot{V}(\mathbf{x}(t)) = \\ \mathbf{x}^\top(t)\mathbf{X}^{-1} \cdot \mathrm{Sym}\big(\mathbf{A}(\mathbf{p})\mathbf{X} + \mathbf{B}(\mathbf{p})\mathbf{M}(\mathbf{p})\big)\mathbf{X}^{-1}\mathbf{x}^\top(t)\,, \tag{11}$$

where "Sym" means symmetric term. (11) can be reformulated as:

$$\mathrm{Sym}\big(\mathbf{A}(\mathbf{p})\mathbf{X} + \mathbf{B}(\mathbf{p})\mathbf{M}(\mathbf{p})\big) = \\ \sum_{i=1}^{R}\sum_{j=1}^{R} w_i(\mathbf{p})w_j(\mathbf{p})\mathrm{Sym}\big(\mathbf{A}_i\mathbf{X} + \mathbf{B}_i\mathbf{M}_j\big) \prec \mathbf{0}\,. \tag{12}$$

The applied parameter dependent convex weighting function $\mathbf{w}(\mathbf{p}(t))$ is the same in case of the system and controller description, which allows the use PDC controller structure (Tanaka and Wang (2001); Baranyi et al. (2013)).

For continuous polytopic LPV systems, the quadratically stabilizing PDC can be constructed by solving the following LMI optimization problem:

$$\begin{gathered}\mathbf{X} \succ \mathbf{0},\\ -\mathbf{X}\mathbf{A}_i^\top - \mathbf{A}_i\mathbf{X} + \mathbf{M}_i^\top\mathbf{B}_i^\top + \mathbf{B}_i\mathbf{M}_i \succ \mathbf{0},\\ -\mathbf{X}\mathbf{A}_i^\top - \mathbf{A}_i\mathbf{X} - \mathbf{X}\mathbf{A}_j^\top - \mathbf{A}_j\mathbf{X}\\ +\mathbf{M}_j^\top\mathbf{B}_i^\top + \mathbf{B}_i\mathbf{M}_j + \mathbf{M}_i^\top\mathbf{B}_j^\top + \mathbf{B}_j\mathbf{M}_i \succeq \mathbf{0},\\ i < j \le R \ \ s.t.\ \forall \mathbf{p}(t) : w_i(\mathbf{p}(t))w_j(\mathbf{p}(t)) = 0\end{gathered} \quad , \tag{13}$$

where $\mathbf{M}_i^{m \times n}$ is the supplementary matrix, $\mathbf{X}^{n \times n}$ is a symmetric, positive definite matrix, while w_i and w_j are general polytopic weighting functions. The belonging control gain (9) is calculated as: $\mathbf{M}_i = \mathbf{G}_i\mathbf{X}$; therefore, $\mathbf{G}_i = \mathbf{M}_i\mathbf{X}^{-1}$ (Tanaka and Wang (2001)).

We have applied control input limitation, since the physiological reality requires the limitation of the amount of the injectable drug. Similarly to (13), this property can be formulated in the form of LMIs as follows (Boyd et al. (1994)):

$$\min_{\mathbf{X},\mathbf{M}} \mu \\ \mathbf{X} \succeq \mathbf{I} \qquad \begin{bmatrix}\mathbf{X} & \mathbf{M}^\top\\ \mathbf{M} & \mu^2\mathbf{I}\end{bmatrix} \succeq \mathbf{0}\,, \tag{14}$$

where is guaranteed that $\|\mathbf{u}(t)\|_2 \le \mu$ at $t \ge 0$. For polytopic cases this holds, if $\mathbf{x}(0)$ lies on the polytope, which is satisfied, if $\|\mathbf{x}(t_0)\|_2 \le 1$. The minimization problem can be extended to μ, if $\|V(\mathbf{x}(t_0))\|_2 \le 1$. The (13)–(14) optimization problem have been applied on Model-B from (6) and have been solved by using the YALMIP framework (Löfberg (2004)) and MOSEK solver (MOSEK ApS (2015)).

Remark 2. Both (14) and EKF design requires preliminary knowledge about the states. The use of different starting points do not cause stability issues due to the slow sampling time. Moreover, the initial tumor size is assumed to be known.

Remark 3. We assumed that $\mathbf{u}(t) \geq 0$ in accordance with the physiological reality: negative control signal, i.e. drug aspiration from blood is not possible.

3.3 Kalman Filter Design

We have developed a continuous/discrete (mixed) EKF (Grewal and Andrews (2008)). The physiological system is continuous, however, we have considered discrete time measurements. It has to be noted that we have applied the Model-A LPV model from (4). The considered sampling time was considered $T = 1$ day in conformity with (1).

The considered model for the EKF was the following:

$$\begin{array}{c} \dot{\mathbf{x}}(t) = f(\mathbf{x}(t), \mathbf{u}(t)) + \mathbf{d}(t), \quad \mathbf{d}(t) \sim \mathcal{N}(\mathbf{0}, \mathbf{Q}(t)) \\ \mathbf{y}_k = h(\mathbf{x}_k) + \mathbf{v}_k, \quad \mathbf{v}_k \sim \mathcal{N}(\mathbf{0}, \mathbf{R}_k) \end{array}. \quad (15)$$

where $f = \mathbf{A}_A(\mathbf{p}(t))\mathbf{x}(t) + \mathbf{B}_A\mathbf{u}(t)$ originates from (4) and $\mathbf{x}_k = \mathbf{x}(t_k)$, while $\mathbf{d}(t)$ represents the system's disturbance, $\mathbf{v}_k = v_k$ is the system's noise and $h = C_A\mathbf{x}_k + \mathbf{v}_k$ is the sensor model.

We have considered additive system disturbances and noise as $d_1(t) \sim \mathcal{N}(0, 5^2)$, $d_2(t) \sim \mathcal{N}(0, 0.5^2)$, $v(k) \sim \mathcal{N}(0, 20^2)$. This results in $\mathbf{Q}(t) = \mathrm{cov}([d_1(t), d_2(t)]^\top)$ and $\mathbf{R}_k = \mathrm{cov}(v(k))$ accordingly. The applied variances are arbitrarily selected (in the lack of available sensor technology), but in accordance with the phenomena.

The initial conditions have been considered the followings: $\hat{\mathbf{x}}_{0|0} = \mathrm{E}\big[\mathbf{x}(t_0)\big]$ and $\mathbf{P}_{0|0} = \mathrm{Var}\big[\mathbf{x}(t_0)\big]$.

The a-priori (prediction) phase can be solved by the following differential equations and by considering that $\hat{\mathbf{x}}(t_{k-1}) = \hat{\mathbf{x}}_{k-1|k-1}$ and $\mathbf{P}(t_{k-1}) = \mathbf{P}_{k-1|k-1}$:

$$\begin{array}{c} \dot{\hat{\mathbf{x}}}(t) = f(\hat{\mathbf{x}}(t), \mathbf{u}(t)) \\ \dot{\mathbf{P}}(t) = \mathbf{F}(t)\mathbf{P}(t) + \mathbf{P}(t)\mathbf{F}^\top(t) + \mathbf{Q}(t) \end{array}, \quad (16)$$

where $\mathbf{F}(t) = \left.\dfrac{\partial f}{\partial \mathbf{x}}\right|_{\hat{\mathbf{x}},\mathbf{u}}$. The solution of (16) is applied in the a-posteriori (update) phase as: $\hat{\mathbf{x}}_{k|k-1} = \hat{\mathbf{x}}(t_k)$ and $\mathbf{P}_{k|k-1} = \mathbf{P}(t_k)$.

The Kalman gain $\mathbf{K}_k$ can be calculated as follows:

$$\mathbf{K}_k = \mathbf{P}_{k|k-1}\mathbf{H}_k^\top(\mathbf{H}_k\mathbf{P}_{k|k-1}\mathbf{H}_k^\top + \mathbf{R}_k)^{-1}, \quad (17)$$

where $\mathbf{H}_k = \left.\dfrac{\partial h}{\partial \mathbf{x}}\right|_{\hat{\mathbf{x}}_{k|k-1}}$.

Next, the following difference equation has to be solved, where $\mathbf{I}$ is the identity matrix in appropriate dimension:

$$\begin{array}{c} \hat{\mathbf{x}}_{k|k} = \hat{\mathbf{x}}_{k|k-1} + \mathbf{K}_k(\mathbf{y}_k - h(\hat{\mathbf{x}}_{k|k-1})) \\ \mathbf{P}_{k|k} = (\mathbf{I} - \mathbf{K}_k\mathbf{H}_k)\mathbf{P}_{k|k-1} \end{array}. \quad (18)$$

3.4 Control Structure

Figure 1 shows the final control structure. We have considered the original model as reference model in this study. In our future work we will investigate other reference models as well.

During the study we have applied constant $u_{ref}(t) = u_{ref}$ reference control signal with appropriately provided reference trajectories $\mathbf{x}_{ref}(t)$. To calculate the necessary u_{ref} two considerations have been done. In order to keep the controllability of Model-B we have taken into account that $u_{ref} > c \cdot (a/b + 10^{-3})$ as a consequence of the model properties. This lead to $x_{2,ref} = p_1 \geq a/b + 10^{-3}$. Our aim was to reach that $x_1 < 1$ [mm^3] over the simulated time horizon. To satisfy these requirements we have calculated u_{ref} as $u_{ref} = c \cdot (a/b + d)$, where $d = 12$ guarantees the $x_{1,ref} < 1$ [mm^3] – which leads that $x_1(t_{final}) < 1$ due to the control framework. The additional d term was arbitrarily selected in conformity with the requirements.

The developed TP-LPV-LMI controller enforced the original nonlinear model to act as the selected reference model. Hence, $\mathbf{x}(t) = \mathbf{x}_{ref}(t)$, $t \to \infty$, which is the same as $\Delta\mathbf{r} = \mathbf{x} - \mathbf{x}_{ref} = \mathbf{0}$.

The unmeasurable state was estimated by the EKF. We have applied $\Delta\hat{\mathbf{x}}(t) = \hat{\mathbf{x}}(t) - \mathbf{x}_{ref}(t)$ for error signal generation, which was compared to $\Delta\mathbf{r} = \mathbf{0}$ as $\Delta\mathbf{e}(t) = \Delta\mathbf{r} - \Delta\hat{\mathbf{x}}(t)$.

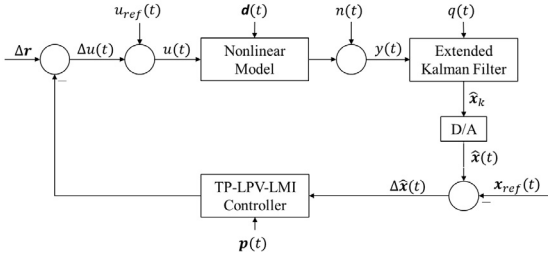

Figure 1. Structure of the control loop.

4. RESULTS

We have used Euler approximation during the simulations with $T = 1$ day sampling time. The sampling density of the parameter vector $\mathbf{p}(t)$ in the parameter domain $\boldsymbol{\Omega}$ was $\mathbf{s} = [199, 199]^\top$ – this sampling density provides good approximation of the original model according to our previous test.

Since $x_1(t)$ was assumed to be measurable, we considered that $x_1(t_0) = 30000$ [mm^3] is available. The inhibitor level is zero before the beginning of the therapy, thus $x_2(t_0) = 0$ [mg/kg]. The reference model has been considered as known and valid. In this way, its initial states can be arbitrarily – but reasonably – determined. We assumed that $x_{1,ref}(t_0) = 30120$ [mm^3] (which is similar to $x_1(t_0)$, but loaded with smaller initial noise with arbitrarily assumed 120 [mm^3]) and $x_{2,ref}(t_0) = a/b + 10^{-3} = 36.4875$ [mg/kg] is the consequence of the model properties and the assumed $p_{1,min}$. The initial states of the EKF have selected by taking into account the aforementioned facts about the reference model and the inhibitor level before the beginning of the therapy: $\hat{x}_1(t_0) = 30120$ [mm^3] and $\hat{x}_2(t_0) = 0$ [mg/kg].

The obtained final states were: $\mathbf{x}(t_{final}) = [0.001,\ 48.2326]^\top$, $\hat{\mathbf{x}}(t_{final}) = [0.005,\ 48.2439]^\top$ and $\mathbf{x}_{ref}(t_{final}) = [0.001, 48.2196]^\top$. The similarity of $\mathbf{x}(t_{final})$ and $\mathbf{x}_{ref}(t_{final})$ indicates the "goodness" of the control.

We assumed additional system disturbances ($d_1(t)$ and $d_2(t)$) and we considered random additive measurement noise v_k. As to our best knowledge, there is no available tumor "sensor", the magnitudes of the disturbances and noises have been arbitrarily selected to be comparable to the magnitude of the states and output. We have taken into account these unfavorable effects during the EKF design.

Figure 2 shows the trajectories of state variables of the original nonlinear model (upper part), EKF (middle part) and reference model (lower part). It is clearly visible that the TP-LPV-LMI based controller enforced the model to behave as the reference model and the EKF approached the original model appropriately as well.

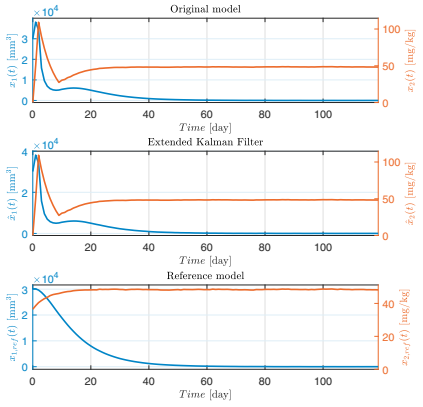

Figure 2. Trajectories of the state variables of the original nonlinear model, EKF and reference model.

Figure 3 strengthen the aforementioned conclusions. The upper part represents the state error related to $\mathbf{x}(t) - \hat{\mathbf{x}}(t)$. It can be seen that the $d_1(t)$ and $d_2(t)$ additive system disturbances reflected in the difference of the states. Despite the disturbances, the EKF was stable. The second subfigure shows the 2-norm based error as $\|\mathbf{x}_{ref}(t) - \mathbf{x}(t)\|_2$, which is a concise description of the state error. At the beginning, the state deviances caused higher error, but due to the appropriate control action the difference decreased until 0.0131 at the end of the simulated time period. The third and fourth subfigures represent the error between the reference model and EKF as $\|\mathbf{x}_{ref}(t) - \hat{\mathbf{x}}(t)\|_2$ from day 0 to 70 and from day 70 to 120, respectively. Similarly to the previous case, the error in 2-norm sense decreased promptly after the higher period at the beginning. The disturbances and sensor noise are not visible due to the magnitude of the initial error. The lowest subfigure shows that despite the appeared disturbances and sensor noise, the EKF approached the reference system appropriately.

Figure 4 shows the $u_{ref}(t)$ reference (upper subfigure) and $u(t)$ realized (middle subfigure) control signals, respectively. The lowest subfigure shows the deviation between the control signals in sense of $u_{ref}(t) - u(t)$.

As we already mentioned, the u_{ref} was considered constant. The middle figure shows that there is a higher peak in $u(t)$ at the beginning. This is a consequence of the state-feedback kind control action due to the initial state

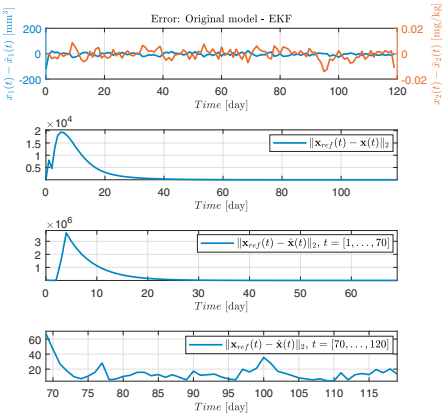

Figure 3. Deviations between the states of the models.

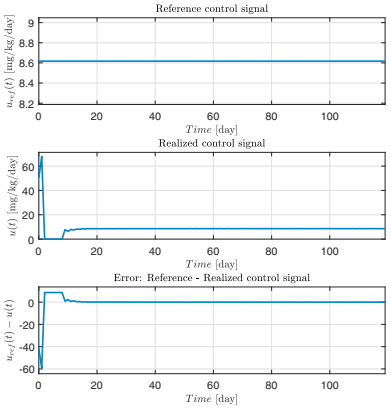

Figure 4. The reference and realized control signals.

discrepancy. After day 18 the deviation between $u_{ref}(t)$ and $u(t)$ was $u_{ref}(t) - u(t) < 0.1$ [mg/kg/day].

During the simulated time horizon the totally injected inhibitor related to the reference controller was $U_{ref} = 1034.1$ [mg/kg]. In contrast, the totally injected inhibitor related to the realized controller was $U = 1067.6$ [mg/kg]. Hence, the deviation between the total amount of inhibitor was $U - U_{ref} = 33.4994$ [mg/kg].

5. CONCLUSIONS

The study introduced the latest achievements regarding the automated control of tumor growth by using angiogenic inhibition.

The mathematical model applied consists of two states representing the tumor growth dynamics under antiangiogenic therapy. We have assumed that $x_1(t)$ is measurable directly. However, the second state needed to be estimated. We have implemented a mixed continuous/discrete EKF – which frequently appears in the literature regarding physiological systems – based on a simple LPV model.

For control design purposes we have developed an error dynamics based LPV model transformed into TP model form. The controller design was done by considering this model and by applying Lyapunov's second law and control

input saturation through LMIs related to polytopic LPV models.

In this study, the original model has been considered as reference system. By using permanent reference control signal, the reference state trajectories were generated by it. The reference control signal was calculated in order to drive the reference states into the desired values.

The validation showed that the developed TP-LPV-LMI controller was able to provide appropriate control action despite the disturbances and noise. The control goal, namely, the tumor volume of the controlled system deceased under a certain – satisfactory – level.

As further step will investigate the use of other tumor growth models in the developed control framework to examine its capabilities. Moreover, we will develop more advanced reference generation possibilities in our future work, analyzing possibilities of reduced parameter uncertainty Precup et al. (2017), the separation of the EKF and controller design and investigating the optimal controller design through the presented framework.

ACKNOWLEDGEMENTS

The Authors thankfully acknowledge the support of the Robotics Special College of Óbuda University.

REFERENCES

Abdalla, A.M., Xiao, L., Ullah, M.W., Yu, M., Ouyang, C., and Yang, G. (2018). Current challenges of cancer anti-angiogenic therapy and the promise of nanotherapeutics. *Theranostics*, 8(2), 533–548.

Baranyi, P., Yam, Y., and Varlaki, P. (2013). *Tensor Product Model Transformation in Polytopic Model-Based Control*. Series: Automation and Control Engineering. CRC Press, Boca Raton, USA, 1st edition.

Boyd, S., El Ghaoui, L., Feron, E., and Balakrishnan, V. (1994). *Linear Matrix Inequalities in System and Control Theory*, volume 15 of *Studies in Applied Mathematics*. SIAM, Philadelphia, PA.

Charlton, P. and Spicer, J. (2016). Targeted therapy in cancer. *Medicine*, 44(1), 34–38.

Drexler, D., Sápi, J., and Kovács, L. (2017a). A minimal model of tumor growth with angiogenic inhibition using bevacizumab. In *SAMI 2017 - IEEE 15th International Symposium on Applied Machine Intelligence and Informatics*, 185–190.

Drexler, D., Sápi, J., and Kovács, L. (2017b). Potential Benefits of Discrete-Time Controller-based Treatments over Protocol-based Cancer Therapies. *Acta Pol Hung*, 14(1), 11–23.

Drexler, D., Sápi, J., and Kovács, L. (2017c). Modeling of tumor growth incorporating the effects of necrosis and the effect of bevacizumab. *Complexity*, 2017, 1–10.

Drexler, D., Sápi, J., and Kovács, L. (2017d). Positive nonlinear control of tumor growth using angiogenic inhibition. *IFAC-PapersOnLine*, 50(1), 15068–15073.

Galambos, P. and Baranyi, P. (2015). TP model transformation: A systematic modelling framework to handle internal time delays in control systems. *Asian J Control*, 17(2), 1–11.

Grewal, M. and Andrews, A. (2008). *Kalman Filtering: Theory and Practice Using MATLAB*. John Wiley and Sons, Chichester, UK, 3rd edition.

Hedrea, L., Bojan-Dragos, C., Precup, R., and Teban, T. (2017). Tensor product-based model transformation for level control of vertical three tank systems. In *2017 IEEE 21st International Conference on Intelligent Engineering Systems (INES)*, 000113–000118. IEEE.

Klamka, J., Maurer, H., and Swierniak, A. (2017). Local controllability and optimal control for amodel of combined anticancer therapy with control delays. *Math Biosci Eng*, 14(1), 195–216.

Kovács, L. (2017). Linear parameter varying (LPV) based robust control of type-I diabetes driven for real patient data. *Knowl-Based Syst*, 122, 199–213.

Kuti, J., Galambos, P., and Baranyi, P. (2017a). Control analysis and synthesis through polytopic tensor product model: a general concept. *IFAC-PapersOnLine*, 50(1), 6558–6563.

Kuti, J., Galambos, P., and Baranyi, P. (2017b). Minimal volume simplex (MVS) convex hull generation and manipulation methodology for TP model transformation. *Asian J Control*, 19(1), 289–301.

Lobato, F., Machado, V., and Steffen, V. (2016). Determination of an optimal control strategy for drug administration in tumor treatment using multi-objective optimization differential evolution. *Comp Meth Prog Biomed*, 131, 51–61.

Löfberg, J. (2004). YALMIP : A Toolbox for Modeling and Optimization in MATLAB. In *In Proceedings of the CACSD Conference*. Taipei, Taiwan.

MOSEK ApS (2015). *The MOSEK optimization toolbox for MATLAB manual. Version 7.1 (Revision 28)*. URL `http://docs.mosek.com/7.1/toolbox/index.html`.

Precup, R., David, R., and Petriu, E. (2017). Grey wolf optimizer algorithm-based tuning of fuzzy control systems with reduced parametric sensitivity. *IEEE T Industr Electr*, 64(1), 527–534.

Sápi, J. (2015). *Controller-managed automated therapy and tumor growth model identification in the case of antiangiogenic therapy for most effective, individualized treatment*. Ph.D. thesis, Applied Informatics and Applied Mathemathics Doctoral School, Óbuda University, Budapest, Hungary.

Sename, O., Gáspár, P., and Bokor, J. (2013). Robust control and linear parameter varying approaches, application to vehicle dynamics. volume 437 of *Lecture Notes in Control and Information Sciences*. Springer-Verlag, Berlin.

Tanaka, K. and Wang, H.O. (2001). *Fuzzy Control Systems Design and Analysis: A Linear Matrix Inequality Approach*. John Wiley and Sons, Chichester, UK, 1st edition.

Vasudev, N. and Reynolds, A. (2014). Anti-angiogenic therapy for cancer: current progress, unresolved questions and future directions. *Angiogenesis*, 17(3), 471–494.

White, A., Zhu, G., and Choi, J. (2013). *Linear Parameter Varying Control for Engineering Applicaitons*. Springer, London, 1st edition.

Xing, K. and Lisong, S. (2017). Molecular targeted therapy of cancer: The progress and future prospect. *Front Lab Med*, 1(2), 69–75.